*Immunology & Cell Biology* 2019; **97**: 726–739
www.wileyonlinelibrary.com/journal/icb

ORIGINAL ARTICLE

# Enhanced safety and immunogenicity of a pneumococcal surface antigen A mutant whole-cell inactivated pneumococcal vaccine

Shannon C David[1], Zoe Laan[1], Vikrant Minhas[1], Austen Y Chen[1], Justin Davies[2], Timothy R Hirst[1,3,4], Shaun R McColl[1], Mohammed Alsharifi[1,3,4,a] & James C Paton[1,3,a]

1 Research Centre for Infectious Diseases, and Department of Molecular and Biomedical Science, School of Biological Sciences, University of Adelaide, Adelaide, SA, Australia
2 Australian Nuclear Science and Technology Organisation, Lucas Heights, NSW, Australia
3 GPN Vaccines Pty Ltd, Yarralumla, ACT, Australia
4 Gamma Vaccines Pty Ltd, Yarralumla, ACT, Australia

**Keywords**
gamma-irradiation, mucosal immunity, pneumococcal vaccine, serotype-independent

**Correspondence**
Mohammed Alsharifi or James C Paton, Research Centre for Infectious Diseases, and Department of Molecular and Biomedical Science, School of Biological Sciences, University of Adelaide, Adelaide, SA 5005, Australia.
E-mail: mohammed.alsharifi@adelaide.edu.au or james.paton@adelaide.edu.au

[a]Equal contributors.

Received 3 October 2018; Revised 21 March 2019; Accepted 29 April 2019

doi: 10.1111/imcb.12257

*Immunology & Cell Biology* 2019; **97**: 726–739

## Abstract

Existing capsular polysaccharide-based vaccines against pneumococcal disease are highly effective against vaccine-included serotypes, but they are unable to combat serotype replacement. We have developed a novel pneumococcal vaccine that confers serotype-independent protection, and could therefore constitute a "universal" vaccine formulation. This preparation is comprised of whole un-encapsulated pneumococci inactivated with gamma irradiation (γ-PN), and we have previously reported induction of cross-reactive immunity after nonadjuvanted intranasal vaccination. To further enhance vaccine immunogenicity and safety, we modified the pneumococcal vaccine strain to induce a stressed state during growth. Specifically, the substrate binding component of the *psaBCA* operon for manganese import was mutated to create a pneumococcal surface antigen A (*psaA*) defective vaccine strain. *psaA* mutation severely attenuated the growth of the vaccine strain *in vitro* without negatively affecting pneumococcal morphology, thereby enhancing vaccine safety. In addition, antibodies raised against vaccine preparations based on the modified strain [γ-PN(ΔPsaA)] showed more diversified reactivity to wild-type pneumococcal challenge strains compared to those induced by the original formulation. The modified vaccine also induced comparable protective $T_H17$ responses in the lung, and conferred greater protection against lethal heterologous pneumococcal challenge. Overall, the current study demonstrates successful refinement of a serotype-independent pneumococcal vaccine candidate to enhance safety and immunogenicity.

## INTRODUCTION

*Streptococcus pneumoniae* (i.e. pneumococcus) remains one of the primary causes of bacterial pneumonia worldwide,[1] and has recently become the leading cause of bacterial meningitis in children <5 years of age in the United States.[2] Pneumococcal vaccines based on the external capsular polysaccharide (CPS) are available, and are highly effective against vaccine-included serotypes. However, of the 98 antigenically diverse serotypes identified to date,[3] a limited number are actually included in existing vaccine formulations. This results in the phenomenon of serotype replacement, whereby reduction in carriage of vaccine-included serotypes leaves a vacant niche in the nasopharynx that can be quickly occupied by nonvaccine serotypes. Carriage and disease prevalence due to nonvaccine serotypes then increases,[4–6] and reduces the effect of vaccination on the overall disease burden.[7]

Recent epidemiological data indicate that widespread use of the 13-valent CPS-protein conjugate vaccine 13 (PCV13) has shifted the serotype distribution of invasive pneumococcal disease (IPD) in multiple regions. For example, a 2017 study found that non-PCV13 serotypes accounted for 57.8% of all childhood IPD cases in North America, 45.9% in the Western Pacific region, 28.5% in Latin America and 71.9% in Europe.[8] A meta-analysis of public health data also found non-PCV serotypes are now the major contributors to IPD burden in adults ≥65 years of age in high-income countries.[9] Furthermore, some studies report that PCVs have failed to consistently reduce the rates of pneumococcal meningitis — one of the most severe forms of IPD — because of serotype replacement.[10,11]

One approach to combat serotype replacement is the further expansion of PCV valency, but this is limited by the complexity and cost of manufacture.[12] Additionally, nonencapsulated *S. pneumoniae* (or nontypeable) is now being reported as an emerging human pathogen.[13] Nonencapsulated *S. pneumoniae* strains are primarily isolated in carriage, although they have been detected in patients with non-IPDs such as otitis media and conjunctivitis, and although extremely rare, invasive nonencapsulated *S. pneumoniae* disease has been reported.[13,14] Given the nature of CPS-based vaccines, they will not offer any protection against disease that is potentially caused by nontypeable strains in the future.[15]

Given these shortcomings, the ongoing efforts aim to develop alternative vaccines that are cheaper to produce and afford protection against all pneumococci. Whole-cell–based vaccines present a possible solution, as they can be relatively inexpensively manufactured and present an almost full complement of antigens to the recipient's immune system. We have previously generated a whole-cell *S. pneumoniae* vaccine preparation inactivated with gammairradiation (γ-PN).[16] This vaccine strain does not express any CPS, allowing exposure of conserved surface proteins for the induction of broadly reactive immune responses. Vaccination with γ-PN was shown to confer significant serotype-independent protection in sepsis and pneumonia challenge models.[16,17] Importantly, protection was conferred after intranasal vaccination without using adjuvant, which provides clear advantages in terms of ease and economy of administration, and induces site-specific memory responses. Other groups have also investigated the possibility of using a whole-cell nonencapsulated pneumococcal vaccine to induce serotype-independent protection,[18–20] with a vaccine developed by Malley *et al.* currently undergoing clinical evaluation. However, these alternative vaccines require administration with an adjuvant, which limits administration to parenteral routes.

To further improve the suitability of our γ-PN vaccine candidate for clinical use, an additional attenuating mutation was introduced to enhance vaccine safety, which also led to enhanced immunogenicity and protective efficacy. It is well documented that the survival of *S. pneumoniae* in different niches is dependent on the acquisition of various nutrients, including sugars and metal ions.[21,22] Of particular interest is the *psaBCA* operon, which encodes the ABC-type manganese ($Mn^{2+}$) importer. Whereas mutation of components required for iron, copper, and zinc import are reported to have variable effects on pneumococcal virulence,[23] mutation of pneumococcal surface antigen A (*psaA*) alone has been shown to cause substantial attenuation in multiple *in vivo* disease models.[24–27] Importantly, *psaA* mutants have a complete requirement for $Mn^{2+}$-supplementation for growth,[24,28] and previous studies have indicated that low $Mn^{2+}$ levels can increase the expression of immunogenic choline-binding proteins such as PcpA[27,29]; thus limiting $Mn^{2+}$ might be expected to modify expression of protective antigens and enable production of vaccine candidates with enhanced immunogenicity. Hence, we investigated the possibility of introducing a growth-attenuating *psaA* mutation to our previously published serotype-independent pneumococcal vaccine strain, and tested the effect of this mutation on vaccine safety and efficacy.

## RESULTS

### Construction of the *psaA* mutant *S. pneumoniae* vaccine strain

The pneumococcal (PN) vaccine strain Rx1(ΔLytA, PdT) was generated previously by replacing *ply* with a nontoxic derivative (PdT) and deleting *lytA* in frame.[16] This strain was further modified in the current study by in-frame deletion of *psaA*, to generate Rx1(ΔLytA, PdT, ΔPsaA) [PN(ΔPsaA)]. The progression of gene manipulation for PN and PN(ΔPsaA) is shown in Figure 1a. PCR analysis using flanking primers showed PN lacked the full-length gene for *lytA*, and the further attenuated PN(ΔPsaA) lacked full-length genes for *lytA* and *psaA*. In each case, a truncated PCR product was detected, indicating successful removal of the protein coding region with only the flanking regions remaining. Ply/PdT was present in all the strains as expected. The expression of PdT and lack of LytA and PsaA in PN (ΔPsaA) was also confirmed by western blot (Figure 1b).

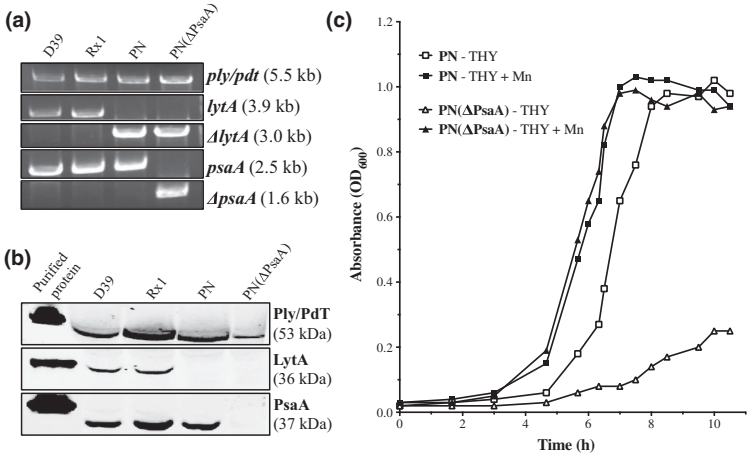


**Figure 1.** Genetic manipulation of pneumococcal vaccine strains. **(a)** Genetic characterization of the vaccine strains Rx1(ΔLytA, PdT) (termed PN) and Rx1(ΔLytA, PdT, ΔPsaA) [termed PN(ΔPsaA)] shown by PCR. **(b)** Western Blot showing Ply/PdT expression in all strains, and lack of LytA and PsaA protein expression in attenuated vaccine strains. Data are representative of two independent experiments. **(c)** *In vitro* growth curves for PN (squares) and PN(ΔPsaA) (triangles) cultured in plain THY media or THY supplemented with 400 μM $MnCl_2$ (THY + Mn). Data indicate mean absorbance ± S.D. ($n$ = 3 biological replicates per strain).

The functional impact of the PsaA deletion on cell growth was then investigated (Figure 1c). The growth curve of the original PN vaccine strain showed a clear log phase, with a transition to stationary phase after roughly 7.5 h. In contrast, dramatically delayed growth kinetics for the modified PN(ΔPsaA) strain were detected when the growth medium (THY) was not supplemented with manganese. However, this growth defect could be repaired by $Mn^{2+}$-supplementation (THY + Mn), with both the strains displaying near-identical growth curves when cultured in this supplemented medium. It was also confirmed that this required $Mn^{2+}$-supplementation had no negative effects on pneumococcal morphology or size (Supplementary figure 1).

### Inactivation of vaccine strains by gamma irradiation

Considering the reported role of $Mn^{2+}$ in altering sensitivity to ionizing radiation,[30–32] we next tested the radiosensitivity of PN and PN(ΔPsaA) vaccine strain after growth in THY with or without additional $Mn^{2+}$. Strains were grown to equivalent $OD_{600}$, extensively washed and exposed to different doses of gamma radiation while frozen on dry ice. Figure 2a, b shows sigmoidal inactivation curves for both the vaccine strains, with an initial area of resistance at low irradiation doses followed by log-linear inactivation. The asymmetric sigmoidal (5PL) nonlinear regression model was used to generate curves of best fit ($R^2 \geq 0.70$ in all cases), and these were used to calculate the dose required for a single $\log_{10}$ reduction in titer ($D_{10}$ value) for each preparation. Data show that the inactivation curves for PN were almost identical regardless of additional $Mn^{2+}$. Interestingly, PN(ΔPsaA) grown in the absence of additional $Mn^{2+}$ exhibited increased sensitivity to gamma irradiation, with a calculated $D_{10}$ value of just 0.37 kGy. Conversely, $D_{10}$ for the same PN (ΔPsaA) strain grown in $Mn^{2+}$-supplemented THY was 0.80 kGy, which closely matches calculated values for both PN preparations (0.82 kGy and 0.75 kGy for PN grown in THY and THY + Mn, respectively).

When using irradiation for pathogen inactivation, the concept of the sterility assurance level (SAL) must be considered. The SAL represents the probability of sterility, and the treatment of medical products routinely requires a SAL of $10^{-3}$ or $10^{-6}$. This indicates that the treatment will reduce bioburden to a theoretical titer below $10^0$ CFU $mL^{-1}$, and corresponds to a one in one thousand or one in one million chance of a single viable microorganism remaining on an item after treatment.[33] To calculate the irradiation dose required to achieve an acceptable SAL for each vaccine preparation, the $D_{10}$ values must be used. Three of the four preparations tested here gave a $D_{10}$ value of ~0.8 kGy. Assuming a starting titer of $10^{11}$ CFU $mL^{-1}$, a total of 11 $\log_{10}$ reductions would be required to reduce the titer to $10^0$ CFU $mL^{-1}$, and a further 6 $\log_{10}$ reductions would achieve the required SAL of $10^{-6}$ CFU $mL^{-1}$. Multiplying the $D_{10}$ value of 0.8 kGy by the total number of 17 $\log_{10}$ reductions required for the SAL gives a final sterilizing

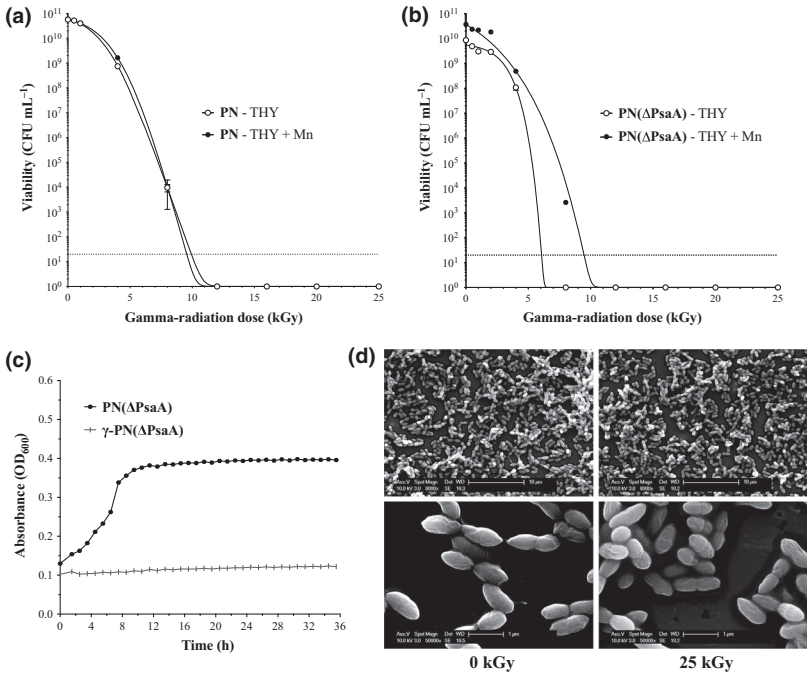


**Figure 2.** Irradiation of vaccine strains. **(a)** PN and **(b)** PN(ΔPsaA) vaccine strains were grown to $OD_{600}$ = 0.65 in THY or THY + Mn, concentrated to ~5 × $10^{10}$ CFU $mL^{-1}$, then exposed to increasing doses of gamma irradiation while frozen on dry ice. CFU counts were used to determine starting titer in nonirradiated (0 kGy) controls, and remaining viable titer in irradiated samples. Data are presented as mean ± S.D. ($n$ = 3 biological replicates per strain per dose). **(c)** Live and irradiated samples of PN(ΔPsaA) were inoculated into SILAC medium + Mn, and $OD_{600}$ of cultures was monitored for 36 h to assess capacity for cell growth. Data are presented as mean $OD_{600}$ ± S.D. ($n$ = 3 biological replicates). **(d)** Representative scanning electron microscopy images (from two independent experiments) of PN(ΔPsaA) samples, either untreated (0 kGy, live controls), or inactivated with 25 kGy of gamma irradiation. Samples were stained with 2% $OsO_4$ prior to progressive dehydration and imaging with a Quanta 450 Scanning Electron Microscope. Samples were viewed at 8000 × magnification (scale bar = 10 μm) and 50 000× magnification (scale bar = 1 μm).

dose of 13.6 kGy. A higher sterilizing dose of 16 kGy was subsequently chosen for vaccine inactivation to further increase the vaccine safety profile by exceeding the SAL required for clinical application. To confirm the sterility of irradiated vaccine preparations, live and 16 kGy-treated PN(ΔPsaA) was cultured in $Mn^{2+}$-supplemented media, and culture density was continually monitored over 36 h. No growth was detected for irradiated PN(ΔPsaA) in comparison to nonirradiated PN(ΔPsaA) (Figure 2c). Additionally, no alteration in cell morphology was observed because of inactivation when exposing vaccine samples to doses as high as 25 kGy (Figure 2d).

## Modulation of innate immune signaling

As pneumococcal morphology was not altered by the ΔPsaA mutation or $Mn^{2+}$-supplementation, we tested whether these modifications could affect innate immune signaling. Live and irradiated samples of each vaccine strain (both grown in THY and THY + Mn) were used to stimulate TLR4- and TLR2-expressing HEK-293 cells. The production of IL-8 by these cells was then quantified as a read-out for the degree of TLR signaling. The IL-8 production in response to stimulation with three different heat-inactivated controls was also included [*Escherichia coli* and *S. pneumoniae* strains D39 (serotype 2), and Rx1 (nonencapsulated D39 derivative)]. Interestingly, our data show that TLR2 signaling induced by the vaccine strains was influenced by both the ΔPsaA mutation and $Mn^{2+}$-supplementation (Figure 3a). Specifically, $Mn^{2+}$-supplementation during growth of the modified PN (ΔPsaA) strain was associated with significantly enhanced TLR2 stimulation, when compared to the original PN strain grown under the same conditions. Additionally, enhancement of TLR2 of signaling by PN(ΔPsaA) grown in $Mn^{2+}$-supplemented medium was observed by both live and irradiated samples, confirming the maintenance of ligands important for innate immune signaling after inactivation by gamma irradiation. Signaling was also higher than the levels triggered by heat-killed Rx1 and

D39, further highlighting the efficacy of irradiation in maintaining the structure of important immune signaling molecules. The IL-8 production by TLR4-expressing HEK cells (Figure 3b) was considerably lower than the TLR2-expressing HEK cells when exposed to the same antigens. Indeed, the levels of IL-8 production in response to all vaccine strains of *S. pneumoniae* was not much higher than the background levels (dotted line). However, as *S. pneumoniae* lacks LPS, which is the main ligand for TLR4 stimulation, the low-level TLR4-mediated signaling was not surprising. By contrast, an *E. coli* heat-killed positive control, elicited approximately double the amount of IL-8 production. *S. pneumoniae* can induce TLR4 signaling via the protein pneumolysin (Ply),[34] which may account for the low-level stimulation seen here. Regardless, the level of TLR4 stimulation between all four vaccine preparations was comparable, with no significant changes in IL-8 production for ΔPsaA strains grown with or without $Mn^{2+}$-supplementation.

### Broader antibody reactivity induced by γ-PN(ΔPsaA)

Our previous studies had demonstrated that B-cell responses against pneumococcal surface antigens are crucial for γ-PN-mediated protection.[16] Interestingly, it was recently shown that naturally acquired immunity to *S. pneumoniae* in humans is also dependent on antibodies against pneumococcal proteins, rather than anti-capsular responses.[35] It was therefore crucial to assess whether anti-protein antibody responses were affected by the modifications to the γ-PN vaccine. Swiss mice were vaccinated twice with equivalent antigen content of γ-PN or γ-PN(ΔPsaA) (both grown in THY and THY + Mn). Pneumococcal-specific IgG and IgA titers were quantified, and we did not detect statistically significant differences in serum and saliva samples across all the vaccinated groups (Supplementary figure 2). The reactivity of serum samples was then tested against whole-cell vaccine lysates using western blot. This allowed further characterization of antibody responses, and comparison of the profile of immunodominant antigens in each vaccine preparation. Remarkably, the modified γ-PN(ΔPsaA) induced antibodies that reacted against a substantially wider range of pneumococcal antigens than those induced by the original γ-PN (Figure 4). The ΔPsaA mutation itself appeared to be responsible for the enhanced reactivity, as illustrated by the diversified banding profile of antibodies induced by γ-PN(ΔPsaA) when compared to γ-PN grown in the same media type. Given the enhanced antibody reactivity and heightened innate signaling (Figure 3b), γ-PN(ΔPsaA) grown in THY + Mn was selected as the optimal version of the pneumococcal vaccine for further investigations.

### Induction of $T_H17$ responses in the lung

In addition to humoral immunity, a role for IL-17 in pathogen clearance has been observed in mouse models for multiple mucosal pathogens.[36,37] It has been shown that mucosal exposure to live bacteria[38] and a killed

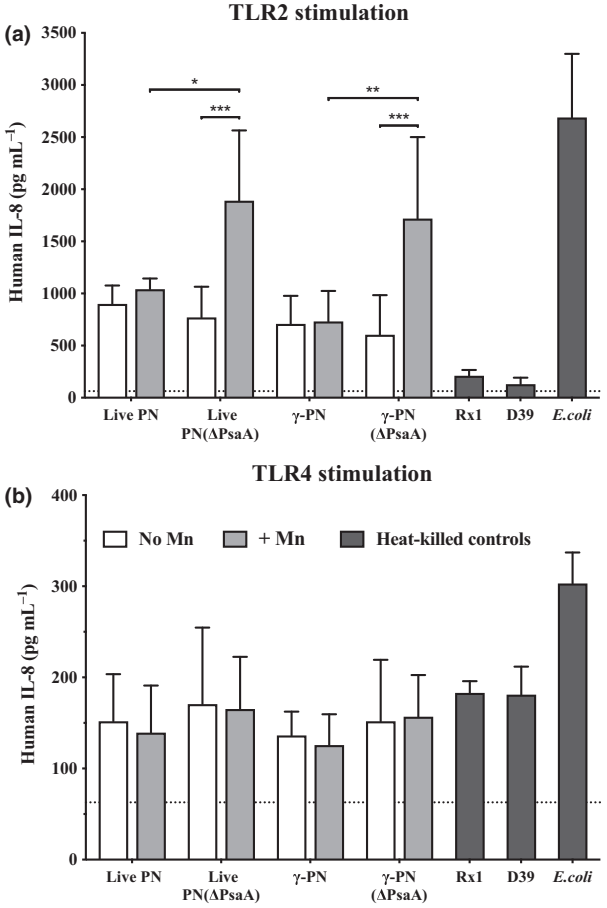


**Figure 3.** $Mn^{2+}$-supplementation of PN(ΔPsaA) is associated with enhanced TLR2 signaling *in vitro*. PN and PN(ΔPsaA) were grown in THY (white bars) or THY + Mn (grey bars), then processed for irradiation. 16 kGy irradiated samples and live 0 kGy control samples of PN and PN(ΔPsaA) were then added to HEK-293 cells stably expressing **(a)** human TLR2, or **(b)** human TLR4. Heat-killed *Escherichia coli*, and heat-killed *S. pneumoniae* strains D39 (serotype 2), and Rx1 (non-encapsulated D39 derivative) were included as positive controls. All antigens were added to cells as whole cell pneumococci, at 10 μg total protein $mL^{-1}$ as determined by bicinchoninic acid. Production of human IL-8 (pg $mL^{-1}$) in culture supernatants after 24 h incubation with antigens was then determined by ELISA. Data are presented as mean IL-8 pg $mL^{-1}$ ± S.D. ($n = 6$ individual culture samples per group), analyzed by two-way ANOVA (*$P < 0.05$; **$P < 0.01$; ***$P < 0.001$). Data compiled from two independent experiments. Dotted line indicates IL-8 production in the absence of any antigen.

un-encapsulated pneumococcal vaccine developed by Malley and co-workers[39] induces immunity against pneumococcal colonization via IL-17A and $CD4^+$ T cell-dependent mechanisms. We have also demonstrated that neutralization of IL-17A abrogates γ-PN-mediated protection against sepsis.[16] Thus, we compared the induction of effector IL-17A-producing T cells (T-helper 17 ($T_H17$) and innate γδ T17 cells) in the lung by the original γ-PN (grown in THY) and the modified γ-PN (ΔPsaA) (grown in THY + Mn). Swiss mice were vaccinated twice prior to challenge with D39. Forty-eight hours post-challenge, lungs were harvested and re-stimulated *ex vivo* to induce cytokine production. Intracellular staining for IL-17 and IFN-γ allowed differentiation of the γδ T-cell subsets T1 and T17, and $CD4^+$ T-cell subsets $T_H1$ and $T_H17$ (flow cytometry gating shown by representative plots in Figure 5a). Interestingly, quantification of γδT17 cells showed no significant enhancement in either vaccine group above the levels detected for phosphate buffered saline (PBS)-mock control mice (Figure 5b). However, a significant decrease in γδT1 cells was detected for both γ-PN- and γ-PN(ΔPsaA)-vaccinated groups compared with controls, suggesting prior vaccination altered the ratio of T17/T1 cells recruited to the lung upon challenge, favoring T17 cells. Data in Figure 5c also demonstrate enrichment of IL-17 –producing $CD4^+$ T cells, with a significant increase in both frequency and total number of $T_H17$ cells in the lungs of γ-PN- and γ-PN(ΔPsaA)-vaccinated mice. A corresponding decrease in $T_H1$ cells was also observed for vaccinated animals compared with controls, although this was only statistically significant for the γ-PN(ΔPsaA)-vaccinated group. Importantly, γδ T-cell and $T_H$ responses were comparable for γ-PN- and γ-PN (ΔPsaA)-vaccinated groups, indicating that ΔPsaA modification of the vaccine strain had no detrimental impact on the induction of protective IL-17 responses.

### The protective efficacy of γ-PN(ΔPsaA)

Initially, we tested the protective immunity induced by the modified γ-PN(ΔPsaA) vaccine against lethal

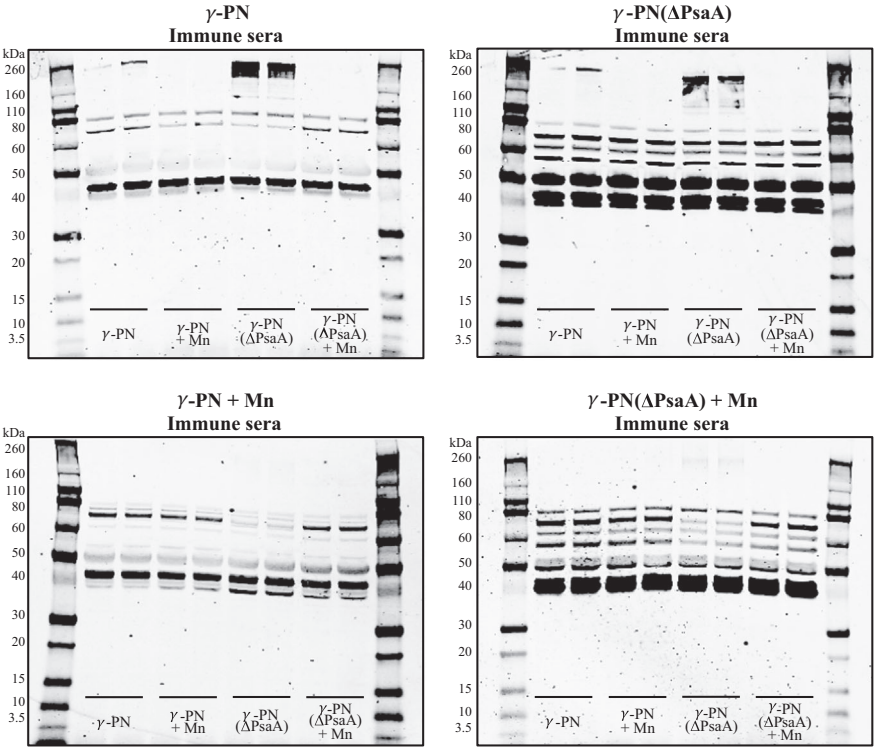


**Figure 4.** Increased reactivity of γ-PN(ΔPsaA)-induced antibody responses against vaccine lysates. Samples of γ-PN and γ-PN(ΔPsaA) vaccines (grown in THY and THY + Mn) were lysed by sonication, and 20 μg total protein loaded per well in duplicate for SDS-PAGE. Separated proteins were transferred to nitrocellulose membranes and probed with immune sera from Swiss mice (pooled sera from 10 individual mice) vaccinated with one of the four vaccine preparations, as indicated. Bound primary IgG was detected using IRDye 800CW goat anti-mouse IgG conjugate, and fluorescence was visualized using a LI-COR Odyssey imaging system. Novex Sharp Pre-Stained Protein Standard was run on all gels for size comparison. Data are representative of two independent experiments.

homologous challenge. Swiss mice received two i.n. vaccinations with γ-PN(ΔPsaA) (grown in THY + Mn) or PBS as a mock vaccine control. Mice were then challenged i.n with a lethal dose of D39 and monitored for survival. As shown in Figure 6a, vaccination with γ-PN(ΔPsaA) induced significant protection against homologous challenge. Furthermore, the survival rate (~50%) of vaccinated animals was similar to that previously observed by Babb *et al.* when testing the original irradiated vaccine against D39.[16] To assess whether the modulated humoral responses induced by γ-PN(ΔPsaA) afforded increased protection, we next compared the efficacy of γ-PN and γ-PN(ΔPsaA) against a severe heterologous challenge. Swiss mice were vaccinated with γ-PN (grown in THY) or γ-PN (ΔPsaA) (grown in THY + Mn) prior to challenge with heterologous serotype 6A (P9 strain). Data presented in Figure 6b show that mice vaccinated with γ-PN(ΔPsaA) were significantly protected against this challenge compared to both PBS-mock controls and γ-PN-vaccinated mice. It is worth noting that γ-PN has been shown to be highly protective against homologous and heterologous serotypes in previous studies,[16,17] but the challenge dose utilized here was intentionally increased to maximize detectable differences in vaccine performance. Immune sera from mice vaccinated with the original γ-PN (grown in THY) and the modified γ-PN(ΔPsaA) (grown in THY + Mn) was also tested against whole-cell lysates of each of these encapsulated challenge strains by western blot analysis. Our data show a broader reactivity against both encapsulated challenge strains, as well as the nonencapsulated vaccine preparations by γ-PN(ΔPsaA)-induced antibodies compared with those elicited by γ-PN (Figure 6c).

## DISCUSSION

The current pneumococcal vaccines offer minimal coverage against newly emerging serotypes and nonencapsulated isolates. Additionally, the limited serotype coverage of existing CPS-based vaccines has been reported to drive serotype replacement, which highlights the need for new strategies providing broad-spectrum protection. We have previously described a novel whole-cell gamma-irradiated *S. pneumoniae* vaccine (γ-PN) capable of inducing serotype-independent protection without any requirement for adjuvant.[16] Here, we report further modification to this novel candidate to enhance vaccine immunogenicity and safety in anticipation of clinical testing.

Specifically, an auxotrophic mutant of the existing nonencapsulated vaccine strain was generated via deletion of *psaA*. Numerous studies have revealed that *psaA* mutants have an absolute requirement for $Mn^{2+}$-supplementation for normal growth kinetics *in vitro*.[24,40] This was confirmed in Figure 1c, where the modified vaccine strain PN(ΔPsaA) displayed poor growth when cultured in THY medium alone. The $Mn^{2+}$ concentration in un-supplemented THY is approximately 0.25 μM,[41] and while this allowed minimal levels of growth of the ΔPsaA strain, the concentration within internal body sites such as the blood is estimated at ~20 nM.[42] Thus, while stringent testing will ensure sterility of irradiated materials, in the unlikely event that any PN(ΔPsaA) cells survive the irradiation process, they will be unable to replicate in sterile body sites following vaccine administration. This auxotrophic mutation represents an additional safety feature to our previously reported gamma-irradiated vaccine. Importantly, the growth defect of the modified ΔPsaA strain could be negated by appropriate $Mn^{2+}$-supplementation *in vitro* to facilitate the manufacture of highly concentrated vaccine preparations. Data also demonstrate that $Mn^{2+}$-supplementation had no detectable effect on the cell morphology, cell length or chain formation (Supplementary figure 1). This was an important consideration, as modulating external $Mn^{2+}$ has been reported to affect cell morphology, which could impact vaccine immunogenicity. Martin *et al.* demonstrated that the enzyme PhpP of *S. pneumoniae* can become hyper-activated because of over-metalation by excess $Mn^{2+}$, resulting in reduced phosphorylation status and defects in cell division, leading to elongated and highly chained pneumococci.[43] However, Martin *et al.* employed mutation of the constitutively expressed manganese exporter MntE to cause accumulation of excess intracellular $Mn^{2+}$. While $Mn^{2+}$ may accumulate in our vaccine strains during growth in $Mn^{2+}$-supplemented media, it is unlikely to reach a toxic intracellular level as the MntE exporter remains entirely functional.

Mn has also been reported to affect irradiation susceptibility,[30–32] and consequently vaccine preparations grown with and without additional $Mn^{2+}$ were exposed to increasing radiation doses. Three of the four vaccine preparations tested here gave a $D_{10}$ value of ~0.8 kGy, indicating similar radiosensitivity (Figure 2a, b). Interestingly, the modified ΔPsaA strain grown in un-supplemented THY gave a substantially lower $D_{10}$ value of 0.37 kGy, indicating increased sensitivity to radiation damage. Daly *et al.* demonstrated that accumulation of intracellular Mn is critical to radiation resistance in *Deinococcus radiodurans*, where it acts in detoxification of reactive oxygen species.[30] It was also proposed in follow-up studies that accumulation of $Mn^{2+}$ facilitates formation of $Mn^{2+}$-metabolite complexes within *D. radiodurans* that protect essential enzymes from oxidative damage.[44–47] Ogunniyi *et al.* demonstrated that a *psaA* deletion mutant of D39 accumulated less than a third of the intracellular $Mn^{2+}$ of wild-type cells when

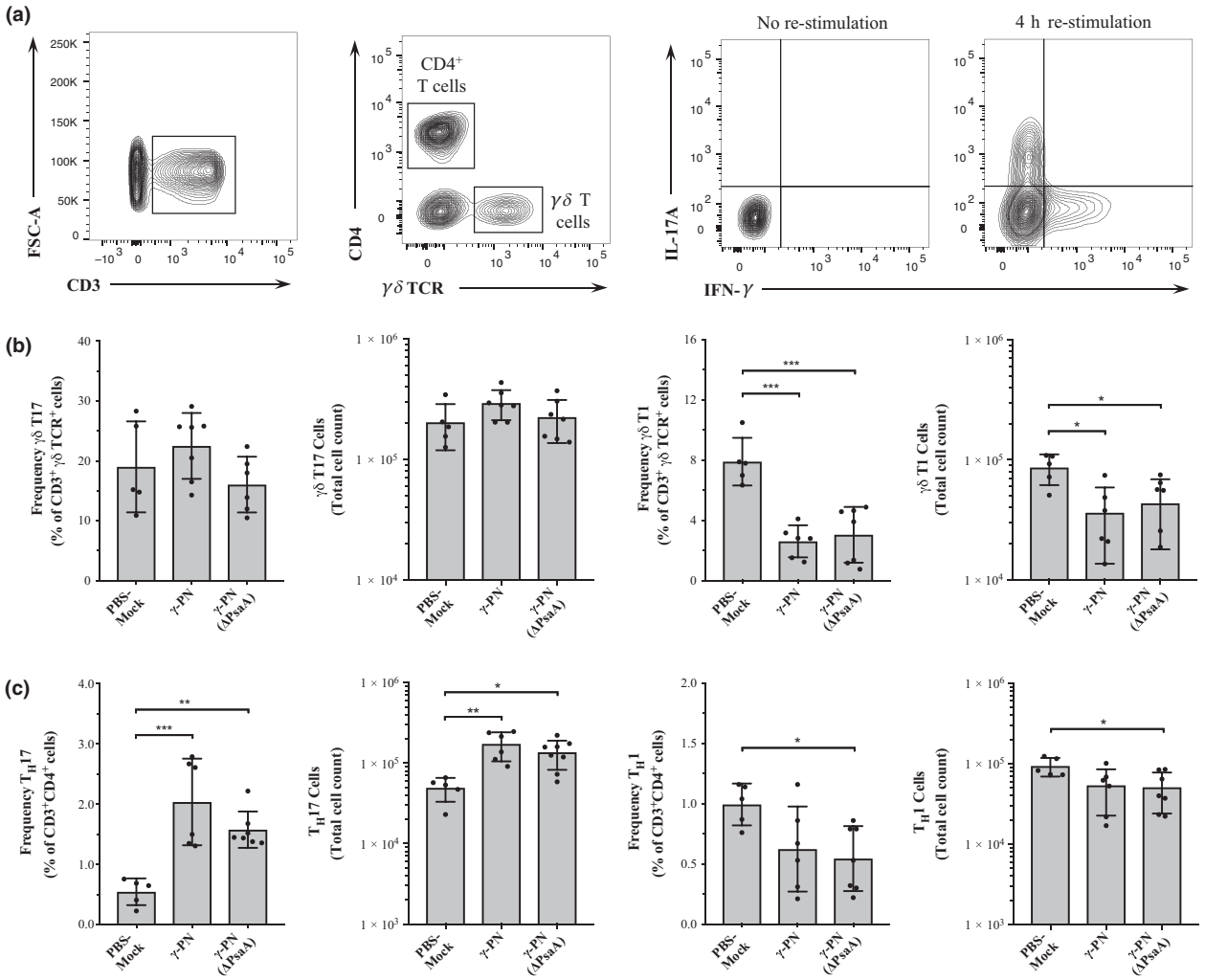


**Figure 5.** Induction of IL-17 producing T-cell subsets after intranasally (i.n.) vaccination. Swiss mice were i.n. vaccinated twice 2 weeks apart with 21.25 μg total protein/dose (~$10^8$ CFU equivalent) of γ-PN or γ-PN(ΔPsaA) (grown in THY and THY + Mn, respectively). Control mice received PBS-mock vaccinations. Two weeks post-second vaccination, mice were challenged i.n. with $10^7$ CFU per mouse of D39 (homologous serotype 2). 48 h later, lungs were harvested for analysis of γδ T cell and $T_H$-cell populations by flow cytometry. **(a)** Representative plots of gating strategy to distinguish γδ T-cells ($CD3^+γδTCR^+$) and $T_H$ cells ($CD3^+CD4^+$). Cells were pre-gated on live/dead and CD44. γδ T-cells and $T_H$ cells were subsequently gated on IL-17A and IFN-γ (induced by *ex vivo* PMA restimulation). **(b)** Frequency and total cell number were quantified for γδT17 ($CD3^+CD44^+γδTCR^+IL\text{-}17A^+$) and γδT1 ($CD3^+CD44^+γδTCR^+IFN\text{-}γ^+$) subsets in vaccinated mice and PBS-mock controls. **(c)** Frequency and total cell number were quantified for $T_H17$ ($CD3^+CD44^+CD4^+IL\text{-}17A^+$) and $T_H1$ ($CD3^+CD44^+CD4^+IFN\text{-}γ^+$) subsets in vaccinated mice and PBS-mock controls. All quantitative data are presented as mean ± S.D. ($n$ = 5 mice for PBS-Mock group, seven mice for each vaccine group), analyzed by one-way ANOVA (*$P$ < 0.05; **$P$ < 0.01; ***$P$ < 0.001).

grown in un-supplemented media,[48] thus lack of this crucial cofactor within the $Mn^{2+}$-starved ΔPsaA vaccine strain is likely to contribute to the enhanced radiosensitivity observed here.

A key factor to consider when modifying our vaccine formulation was the potential alteration to expression of key antigens. We anticipated the induction of a "stressed" protein profile in the *ΔpsaA* vaccine strain due to nonoptimal $Mn^{2+}$ import. High extracellular $Mn^{2+}$ can also influence the expression of genes under the control of *psaR*,[29] including protective immunogens PrtA (extracellular serine protease) and PcpA (choline-binding protein).[27,48–52] Therefore, we tested the immunogenicity of our four different vaccine preparations (γ-PN or γ-PN (ΔPsaA) grown with or without additional $Mn^{2+}$) by analyzing the potency of antibody responses in serum and saliva of vaccinated mice against a whole-cell pneumococcal antigen. Note that this whole-cell antigen was a nonirradiated sample of the original γ-PN vaccine, hence all protective antigens were present on the

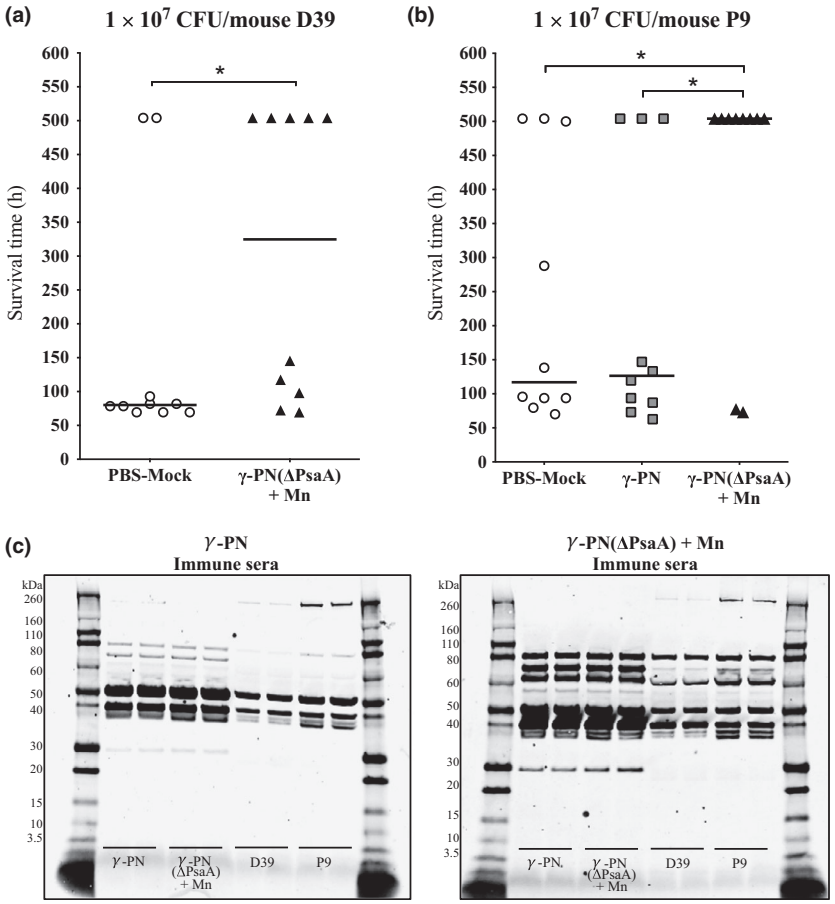


**Figure 6.** Protection against lethal pneumococcal challenge conferred by intranasally (i.n.) vaccination with γ-PN(ΔPsaA). **(a)** Swiss mice were i.n. vaccinated twice, 2 weeks apart with 21.25 μg total protein/dose/mouse (~$10^8$ CFU equivalent/mouse) of γ-PN(ΔPsaA) (grown in THY + Mn). Control mice received PBS-mock vaccinations. Two weeks post-second vaccination, mice were challenged i.n. with $10^7$ CFU per mouse of D39 (homologous serotype 2). **(b)** Mice were i.n. vaccinated twice with 21.25 μg total protein/dose/mouse of either γ-PN (grown in THY) or γ-PN (ΔPsaA) (grown in THY + Mn). Control mice received PBS-mock vaccinations. Two weeks post-second vaccination, mice were challenged i.n. with $10^7$ CFU per mouse of P9 (heterologous serotype 6A). All mice were monitored for 3 weeks for development of clinical symptoms and overall survival. Data points indicate the survival time for each mouse ($n$ = 10 per group), and horizontal bars indicate the median survival time for each group. Differences in survival time were analyzed by Mann–Whitney $U$-test (*$P$ < 0.05). Data are representative of two independent experiments. **(c)** D39 and P9 challenge strains, and γ-PN and γ-PN(ΔPsaA) vaccines (grown in THY and THY + Mn, respectively) were all lysed by sonication, and 20 μg total protein loaded per well in duplicate for SDS-PAGE. Blots were probed with pooled immune sera from vaccinated Swiss mice ($n$ = 10 mice per group), as indicated. Bound primary IgG was detected using IRDye 800CW goat anti-mouse, and fluorescence was visualized using a LI-COR Odyssey imaging system. Novex Sharp Pre-Stained Protein Standard was run for size comparison. Data are representative of two independent experiments.

pneumococcal surface. Data showed no statistical differences in overall titers of IgG and IgA in serum and saliva samples, indicating no loss of key antigens by ΔPsaA mutation nor $Mn^{2+}$ supplementation that would reduce titers detected by ELISA. In fact, the ΔPsaA modification appeared to enhance reactivity of vaccine-induced antibody responses to pneumococcal antigens present in both homologous and heterologous strains (Figures 4 and 6c).

The mechanism behind this modulated antibody diversity is yet to be elucidated. As mentioned previously, it is likely that loss of PsaA functionality increased the expression of certain surface proteins because of stress. Consequently, the range of vaccine antigens recognized and processed *in vivo* may have been larger, resulting in more diverse reactivity of vaccine-induced humoral responses. Alternatively, vaccination with γ-PN(ΔPsaA) may have been associated with an altered cytokine profile in the lung due to modulated innate signaling, which could augment downstream antigen processing. In fact, significantly enhanced TLR2 signaling was detected *in vitro* for the ΔPsaA modified vaccine (Figure 3a). Regardless of

mechanism, the diversified antibody reactivity is likely to be a major factor contributing to the enhanced protection observed for γ-PN(ΔPsaA)-vaccinated animals against severe heterologous challenge (Figure 6b).

$T_H17$ populations in the lung were also comparable between γ-PN- and γ-PN(ΔPsaA)-vaccinated mice (Figure 5), indicating no loss of key antigens required for IL-17 responses after intranasal vaccination. This is crucial for ongoing development of our intranasally (i.n.)-delivered vaccine. In general, bacteria-like particles such as our whole-cell vaccine preparation have an advantage at inducing mucosal immunity.[53,54] Due to presentation of pneumococcal antigens and activation of toll-like receptors, whole-cell antigens are better processed for immunity, whereas soluble antigens tend to elicit tolerance.[55] Previous studies have also established that intranasal inoculation is superior for induction of $T_H17$ responses in the lung when compared with parenteral routes (intraperitoneally, i.v., s.c.),[56–59] and mucosal $T_H17$ responses are strongly associated with protection against pneumococcal colonization[60] and development of pneumonia.[61,62]

However, for many whole-inactivated vaccine preparations their method of inactivation requires that an adjuvant is coadministered in order to elicit significant mucosal responses, which limits their suitability for intranasal administration and induction of lung-specific immunity. For example, the whole-cell vaccine originally developed by Malley *et al.* was intended for intranasal administration.[18] Their initial studies demonstrated that protection against serotype 3 pneumonia, and reduced nasopharyngeal and middle ear colonization after intranasal vaccination was dependent on the use of cholera toxin and *Escherichia coli* heat-labile toxin as adjuvants.[18,20,63] The clinical experience with labile toxin[64] and a singly mutated derivative, labile toxin-K63,[65] has revealed several cases of Bell's palsy when these adjuvants are given i.n., which has raised concerns about the use of toxin-adjuvanted vaccines for human use via this route. By contrast, γ-PN induces broadly reactive immunity without the need for any adjuvant, implying that our vaccine preparation may be more suitable for intranasal use in humans for the induction of strong lung-specific memory responses.

Overall, the modification to our vaccine strain has further heightened the vaccine safety profile, and enhanced the reactivity of vaccine-induced antibody responses. Induction of lung $T_H17$ responses following mucosal vaccination without any adjuvant also ensures our new formulation is still suitable for intranasal vaccination in a clinical setting. Furthermore, the induction of systemic antibodies with broader reactivity is likely to mediate enhanced complement deposition and opsonophagocytosis of invading heterologous pneumococci, facilitating clearance of infection and superior serotype-independent protection.

## METHODS

### Ethics statement

Animal experimentation was carried out in strict accordance with the Australian Code of Practice for Care and Use of Animals for Scientific Purposes [7th edition (2004) and 8th edition (2013)] and the South Australian Animal Welfare Act 1985. Experimental protocols were approved by the Animal Ethics Committee at The University of Adelaide (Approval numbers S-2013-053 and S-2016-183).

### Construction of the Rx1(ΔLytA, PdT, ΔPsaA) vaccine strain

*Streptococcus pneumoniae* strains statically grown in Todd–Hewitt broth + 0.5% yeast extract (THY) at 37°C in 5% $CO_2$ unless otherwise stated. The *S. pneumoniae* strain Rx1 is a capsule-deficient derivative of D39 (serotype 2), and the generation of isogenic mutant Rx1(ΔLytA, PdT) (termed PN) was previously described.[16] Additional genetic manipulation was performed to delete the *psaA* gene in-frame, in a similar manner as described previously.[66] PCR primers are listed in Supplementary table 1. A tagged *psaA* deletion mutant was generated by the transformation of Rx1(ΔLytA, PdT) with a cassette comprising an erythromycin resistance gene ($Ery^R$) fused to *psaA* 5′ and 3′ flanking regions. THY supplemented with 400 μM $MnCl_2$ (THY + Mn) was used for all transformation steps and subsequent growth steps with the resulting Rx1(ΔLytA, PdT, ΔPsaA::$Ery^R$) strain, to overcome the growth defect of PsaA-null mutants. A PCR product that fused *psaA* 5′ and 3′ flanking regions was then generated, and used to replace the $Ery^R$ cassette in Rx1(ΔLytA, PdT, ΔPsaA::$Ery^R$), deleting *psaA* in-frame. Transformants were screened for loss of erythromycin resistance by replica plating. *psaA* flanking regions of putative mutants were PCR amplified, and in-frame deletions confirmed by Sanger sequencing. The final Rx1(ΔLytA, PdT, ΔPsaA) strain [termed PN(ΔPsaA)] was additionally validated using PCR and western Blot.

### Generation of γ-irradiated vaccines

PN and PN(ΔPsaA) vaccine strains were inoculated from blood agar plates into THY or THY + Mn to a starting $OD_{600}$ of 0.02. Cultures were incubated at 37°C + 5% $CO_2$ until $OD_{600}$ = 0.65. Cells were pelleted by centrifugation at 4000× *g* for 10 min at 4°C, washed three times in PBS, and resuspended in PBS + 13% glycerol to ~$10^{10}$ CFU $mL^{-1}$ (100 × concentration from original volume). Two hundred microliter aliquots of PN and PN(ΔPsaA) vaccines were inactivated by exposure to γ-irradiation by the Australian Nuclear Science and Technology Organization (Lucas Heights, NSW, Australia). Samples were kept frozen on dry ice during irradiation and transportation.

Remaining viable titers were determined by CFU counts on blood agar plates. Based on inactivation curves, a sterilizing dose of 16 kGy was used for vaccine inactivation, generating γ-PN and γ-PN(ΔPsaA). The sterility of 16 kGy-irradiated vaccines was confirmed by plating of neat samples.

## Bacterial growth

Live PN and PN(ΔPsaA) strains were inoculated into THY and THY + Mn as described previously, and $OD_{600}$ measured every 30–60 min for 10 h. For additional testing of sterility after irradiation, live and 16 kGy-treated PN(ΔPsaA) samples were inoculated from frozen aliquots into SILAC media + 0.5% glucose + 400 μM $MnCl_2$ to $OD_{600}$ = 0.1. Cultures were incubated at 37°C + 5% $CO_2$ and $OD_{600}$ regularly monitored for 36 h.

## Scanning electron microscopy

Live PN and PN(ΔPsaA) strains were inoculated from blood agar plates into 100 mL THY or THY + Mn to a starting $OD_{600}$ of 0.02. Cultures were incubated at 37°C + 5% $CO_2$, and 25 mL samples were removed at $OD_{600}$ = 0.2, 0.4 and 0.65, then pelleted and washed as described previously. Pellets were resuspended in 250 μL PBS + 13% glycerol (100 × concentration from original volume). A total of 15 μL of neat sample was diluted in 2 mL sterile PBS for transfer to Whatman® Nucleopore Track-Etch polycarbonate membrane filters (GE Healthcare, Parramatta, NSW, Australia). Samples briefly fixed in EM fixative (4% paraformaldehyde, 1.25% glutaraldehyde, 4% sucrose in PBS, pH 7.2) and stained with 2% osmium tetroxide ($OsO_4$) prior to progressive dehydration (as described in Alternate Protocol 6 and Basic Protocol 3[67]). Membranes were air dried, and then coated by gold sputter prior to imaging using a Quanta 450 Scanning Electron Microscope at Adelaide Microscopy, University of Adelaide.

### *TLR4 and TLR2 stimulation*

Human embryonic kidney cells (HEK-293) cells stably transfected with human TLR4a gene (293/TLR4a, cat. #293-htlr4a) or human TLR2 and CD14 genes (293/hTLR2-CD14, cat. #293-htlr2 cd14) were obtained from InvivoGen, San Diego, CA, USA. The cells were maintained in Gibco DMEM + 10 mM HEPES, 10% FCS, 1% penicillin/streptomycin, 1% Glutamax, 100 μg $mL^{-1}$ normocin (cat. #ant-nr-1; InvivoGen), and 10 μg $mL^{-1}$ blasticidin (cat. #ant-bl-1, InvivoGen). For stimulation, cells were seeded in 24-well plates at $3 \times 10^5$ cells per well in 0.5 mL culture medium, and incubated for ~24 h until confluent. Culture medium was removed, and replaced with 0.3 mL of assay medium (culture medium with 1% FCS only) containing whole-cell vaccine antigens at 10 μg $mL^{-1}$ [as determined by bicinchoninic acid (BCA) assay]. Assay medium alone was used to determine background IL-8. After 24 h stimulation, culture supernatants were harvested for determination of IL-8 production by ELISA using the human IL-8/CXCL8 DuoSet ELISA kit (cat. #DY208-05; R&D Systems, Minneapolis, MN, USA) according to the manufacturer's instructions.

### *Mice and treatment*

Female outbred Swiss mice (4–6 weeks old) were obtained from the Laboratory Animal Services at the University of Adelaide, South Australia. Mice were anesthetized intraperitoneally with sodium pentobarbitone at 66 μg $g^{-1}$ body weight. Anesthetized mice were i.n. vaccinated with γ-PN or γ-PN(ΔPsaA) by gently applying 30 μL of the inactivated vaccine preparation (21.25 μg total protein per dose in PBS, ~$10^8$ CFU equivalent per dose) to the nostrils. Control mice received PBS as a mock vaccine. Mice were vaccinated i.n. twice at 2-week intervals. At 1 week post-second vaccination, serum samples were collected by submandibular bleeding, and saliva was harvested after injection of pilocarpine (at 2 mg $mL^{-1}$, 10 μL $g^{-1}$ body weight) intraperitoneally. For challenge experiments, mice were anesthetized as described previously and challenged i.n. 2 weeks post-second vaccination with D39 or P9 ($10^7$ CFU per mouse in 25 μL PBS). Mice were monitored daily for 3 weeks post-challenge for development of clinical symptoms, and humanely euthanized once mice became moribund.

## Measurement of antibody responses

Serum and saliva samples were assayed by ELISA to determine *S. pneumoniae*-specific antibody titers, essentially as described previously.[68] Live whole-cell PN was used as the coating antigen, at $5 \times 10^6$ CFU per well in 100 mM bicarbonate/carbonate buffer (pH 9.6). Alkaline phosphatase conjugated goat anti-mouse IgA (1:1000 dilution; Zymed, San Francisco, CA, USA) and horseradish peroxidase (HRP) conjugated goat anti-mouse IgG (1:10 000 dilution; Thermo-Fisher, Rockford, IL, USA) were used to detect IgA and total IgG, respectively. Color was developed using pNPP disodium hexahydrate tablets (cat. #N9389; Sigma-Aldrich, Castle Hill, NSW, Australia) for Alkaline phosphatase-conjugated antibodies, and the BD OptEIA TMB Substrate kit (Becton Dickinson, North Ryde, NSW, Australia) for horseradish peroxidase conjugates. The absorbance reading of samples from PBS-Mock vaccinated mice were used to calculate the cut-off value for all the antibody titers. The cut-off was calculated by adding the mean absorbance value to 3 × S.D. End-point titers for test samples were then expressed as the reciprocal of the dilution where the absorbance value equaled the cut-off value.

## Analysis of γδ and $CD4^+$ T-cell responses

Mice were i.n. vaccinated twice 2 weeks apart, then challenged i.n with $10^7$ CFU per mouse D39. At 48 h post-challenge, mice were euthanized by $CO_2$ asphyxiation, and perfused with 10 mL cold PBS. Lungs were harvested and finely macerated in 1 mL prewarmed digestion medium [DMEM + 5% FCS, 10 mM HEPES, 2.5 mM $CaCl_2$, 0.2 U $mL^{-1}$ penicillin/gentamicin, 1 mg $mL^{-1}$ collagenase IA (Sigma-Aldrich), 30 U $mL^{-1}$ DNase (Sigma-Aldrich)] and incubated at 37°C for 1 h with mixing every 20 min. Single-cell suspensions were prepared and stained as previously described,[69] using antibodies against surface markers and

intracellular cytokines listed in Supplementary table 2. All stains were washed in PBS 0.04% azide, and resuspended in PBS 1% paraformaldehyde for acquisition on a BD LSRFortessa X20 flow cytometer.

### BCA protein assay

To generate whole-cell lysates, aliquots of each vaccine were diluted 1:10 in PBS, and added to tubes containing 40 mg glass beads (cat. #G4649-10G; Sigma-Aldrich) for sonication at 4°C (25 cycles: 30 s on, 30 s off). Lysates were then separated from the glass beads, and quantified with the Pierce BCA Protein Assay Kit (cat. #2322; Pierce Biotechnology, Rockford, IL, USA) according to the manufacturer's specifications.

### Western blotting

SDS-PAGE and protein transfer was performed using NuPAGE Bis-Tris protein gels, nitrocellulose membranes and the iBlot transfer system (Thermo Fisher, Norwood, SA, Australia) according to the manufacturer's instructions. For confirmation of mutants, the encapsulated parent strain D39, the Rx1 strain, and the vaccine strains PN and PN(ΔPsaA) were grown to mid-log phase, washed in PBS, and concentrated ~50 × by centrifugation. Samples were lysed as described previously, and boiled in 1 × LUG buffer for 5 min at 95°C prior to SDS-PAGE. Immunoblotting was performed using polyclonal murine anti-Ply (1:10 000 dilution), anti-LytA (1:10 000), or anti-PsaA (1:2000). The primary antibodies were detected with goat anti-mouse IgG IRDye800 (1:50 000 dilution; LI-COR, Lincoln, NE, USA) and visualized using the LI-COR Odyssey fluorescent imaging system.

To assess antibody reactivity, whole-cell lysates for both vaccine strains and encapsulated D39 and P9 were generated and quantified as per BCA assay. Lysates were boiled as described previously, and 20 μg total protein per well was used for SDS-PAGE. After transfer, membranes were probed with pooled immune sera from vaccinated Swiss mice (1:500 dilution). Bound antibody was detected and visualized as described previously.

### Statistical analysis

All quantitative results are expressed as mean ± S.D. One-way ANOVA was used for comparison of data from three or more groups involving a single independent variable, and two-way ANOVA was used when data were grouped according to two independent variables. Tukey's multiple comparisons test was used for *post hoc* analysis. For survival data analysis, the Mann–Whitney *U*-test was used, after determination of nonparametric distribution by the D'Agostino & Pearson test and the Shapiro–Wilk test. All analyses were performed using GraphPad Prism 8, version 8.0.1 (GraphPad Software, La Jolla, CA, USA). *P*-values < 0.05 (95% confidence) were considered statistically significant.

## ACKNOWLEDGMENTS

The authors thank Adelaide University Microscopy (Adelaide, Australia) for assisting with operation of the Quanta 450 Scanning Electron Microscope. We also acknowledge the following funding sources supporting this research: an AINSE Research Award (ALNGRA15517; to MA); an Australian Postgraduate Award and Gamma Vaccines Pty Ltd research sponsorship (to SCD); and a NHMRC Senior Principal Research Fellowship and NHMRC Development Grant (to JCP).

## CONFLICT OF INTEREST

GPN Vaccines Pty Ltd owns patents covering the gamma-irradiated pneumococcal vaccines reported in this paper. MA, TRH and JCP are Directors of GPN Vaccines Pty Ltd; and MA, SD, TRH and JCP are shareholders in the company. This does not alter adherence to policies on sharing data and materials.

## REFERENCES

1. World Health Organization (WHO). Fact Sheet—Pneumonia. WHO; 2016.
2. National Center for Immunization and Respiratory Diseases (Division of Bacterial Diseases). *Streptococcus pneumoniae*: Clinical Features. Washington DC: Public Health Foundation; 2015.
3. Geno KA, Saad JS, Nahm MH. Discovery of novel pneumococcal serotype 35D, a natural WciG-deficient variant of serotype 35B. *J Clin Microbiol* 2017; **55**: 1416–1425.
4. Hicks LA, Harrison LH, Flannery B, *et al.* Incidence of pneumococcal disease due to non-pneumococcal conjugate vaccine (PCV7) serotypes in the united states during the era of widespread PCV7 vaccination, 1998-2004. *J Infect Dis* 2007; **196**: 1346–1354.
5. Beall BW, Gertz RE, Hulkower RL, *et al.* Shifting genetic structure of invasive serotype 19A pneumococci in the United States. *J Infect Dis* 2011; **203**: 1360–1368.
6. Sa-Leao R, Nunes S, Brito-Avo A, *et al.* Changes in pneumococcal serotypes and antibiotypes carried by vaccinated and unvaccinated day-care centre attendees in Portugal, a country with widespread use of the seven-valent pneumococcal conjugate vaccine. *Clin Microbiol Infec* 2009; **15**: 1002–1007.
7. Weinberger DM, Malley R, Lipsitch M. Serotype replacement in disease after pneumococcal vaccination. *Lancet* 2011; **378**: 1962–1973.
8. Balsells E, Guillot L, Nair H, *et al.* Serotype distribution of *Streptococcus pneumoniae* causing invasive disease in children in the post-PCV era: a systematic review and meta-analysis. *PLoS ONE* 2017; **12**: e0177113.
9. Izurieta P, Bahety P, Adegbola R, *et al.* Public health impact of pneumococcal conjugate vaccine infant immunization programs: assessment of invasive pneumococcal disease burden and serotype distribution. *Expert Rev Vaccines* 2018; **17**: 479–493.

10. Brouwer MC, van de Beek D. Epidemiology of community-acquired bacterial meningitis. *Curr Opin Infect Dis* 2018; **31**: 78–84.
11. Olarte L, Barson WJ, Barson RM, *et al.* Impact of the 13-valent pneumococcal conjugate vaccine on pneumococcal meningitis in US children. *Clin Infect Dis* 2015; **61**: 767–775.
12. Miller E, Andrews NJ, Waight PA, *et al.* Effectiveness of the new serotypes in the 13-valent pneumococcal conjugate vaccine. *Vaccine* 2011; **29**: 9127–9131.
13. Bradshaw JL, Pipkins HR, Keller LE, *et al.* Mucosal infections and invasive potential of nonencapsulated *Streptococcus pneumoniae* are enhanced by oligopeptide binding proteins AliC and AliD. *MBio* 2018; **9**: e02097–17.
14. Martin CS, Bradshaw JL, Pipkins HR, *et al.* Pulmonary disease associated with nonencapsulated *Streptococcus pneumoniae*. *Open Forum Infect Dis* 2018; **5**: ofy135.
15. Castiglia P. Recommendations for pneumococcal immunization outside routine childhood immunization programs in Western Europe. *Adv Ther* 2014; **31**: 1011–1044.
16. Babb R, Chen A, Hirst TR, *et al.* Intranasal vaccination with gamma-irradiated *Streptococcus pneumoniae* whole-cell vaccine provides serotype-independent protection mediated by B-cells and innate IL-17 responses. *Clin Sci* 2016; **130**: 697–710.
17. Babb R, Chen A, Ogunniyi AD, *et al.* Enhanced protective responses to a serotype-independent pneumococcal vaccine when combined with an inactivated influenza vaccine. *Clin Sci* 2017; **131**: 169–180.
18. Malley R, Lipsitch M, Stack A, *et al.* Intranasal immunization with killed unencapsulated whole cells prevents colonization and invasive disease by capsulated pneumococci. *Infect Immun* 2001; **69**: 4870–4873.
19. Mohammadzadeh M, Pourakbari B, Doosti A, *et al.* Construction and evaluation of a whole-cell pneumococcal vaccine candidate. *J Appl Microbiol* 2018 [Epub ahead of print]. https://doi.org/10.1111/jam.14079.
20. Malley R, Morse SC, Leite LC, *et al.* Multiserotype protection of mice against pneumococcal colonization of the nasopharynx and middle ear by killed nonencapsulated cells given intranasally with a nontoxic adjuvant. *Infect Immun* 2004; **72**: 4290–4292.
21. Bayle L, Chimalapati S, Schoehn G, *et al.* Zinc uptake by *Streptococcus pneumoniae* depends on both AdcA and AdcAII and is essential for normal bacterial morphology and virulence. *Mol Microbiol* 2011; **82**: 904–916.
22. Wakeman CA, Skaar EP. Metalloregulation of Gram-positive pathogen physiology. *Curr Opin Microbiol* 2012; **15**: 169–174.
23. Honsa ES, Johnson MD, Rosch JW. The roles of transition metals in the physiology and pathogenesis of *Streptococcus pneumoniae*. *Front Cell Infect Microbiol* 2013; **3**: 92.
24. Marra A, Lawson S, Asundi JS, *et al. In vivo* characterization of the *psa* genes from *Streptococcus pneumoniae* in multiple models of infection. *Microbiology* 2002; **148**: 1483–1491.
25. Kadioglu A, Weiser JN, Paton JC, *et al.* The role of *Streptococcus pneumoniae* virulence factors in host respiratory colonization and disease. *Nat Rev Microbiol* 2008; **6**: 288–301.
26. Berry AM, Paton JC. Sequence heterogeneity of PsaA, a 37-kilodalton putative adhesin essential for virulence of *Streptococcus pneumoniae*. *Infect Immun* 1996; **64**: 5255–5262.
27. Johnston JW, Briles DE, Myers LE, *et al.* $Mn^{2+}$-dependent regulation of multiple genes in *Streptococcus pneumoniae* through PsaR and the resultant impact on virulence. *Infect Immun* 2006; **74**: 1171–1180.
28. Tseng HJ, McEwan AG, Paton JC, *et al.* Virulence of *Streptococcus pneumoniae*: PsaA mutants are hypersensitive to oxidative stress. *Infect Immun* 2002; **70**: 1635–1639.
29. Manzoor I, Shafeeq S, Kuipers OP. $Ni^{2+}$-dependent and PsaR-mediated regulation of the virulence genes *pcpA*, *psaBCA*, and *prtA* in *Streptococcus pneumoniae*. *PLoS ONE* 2015; **10**: e0142839.
30. Daly MJ, Gaidamakova EK, Matrosova VY, *et al.* Accumulation of Mn(II) in *Deinococcus radiodurans* facilitates gamma-radiation resistance. *Science* 2004; **306**: 1025–1028.
31. Anjem A, Varghese S, Imlay JA. Manganese import is a key element of the OxyR response to hydrogen peroxide in *Escherichia coli*. *Mol Microbiol* 2009; **72**: 844–858.
32. Webb KM, DiRuggiero J. Role of $Mn^{2+}$ and compatible solutes in the radiation resistance of thermophilic bacteria and archaea. *Archaea* 2012; **2012**: 845756.
33. International Organisation for Standardisation (ISO). Establising the Sterilisation Dose (ISO 11137-2:2013(E)). Sterilisation of Health Care Products—Radiation, 3rd edn. Geneva, Switzerland: ISO; 2013.
34. Malley R, Henneke P, Morse SC, *et al.* Recognition of pneumolysin by Toll-like receptor 4 confers resistance to pneumococcal infection. *Proc Natl Acad Sci USA* 2003; **100**: 1966–1971.
35. Wilson R, Cohen JM, Reglinski M, *et al.* Naturally acquired human immunity to pneumococcus is dependent on antibody to protein antigens. *PLoS Pathog* 2017; **13**: e1006137.
36. Curtis MM, Way SS. Interleukin-17 in host defence against bacterial, mycobacterial and fungal pathogens. *Immunology* 2009; **126**: 177–185.
37. O'Connor W Jr, Zenewicz LA, Flavell RA. The dual nature of T(H)17 cells: shifting the focus to function. *Nat Immunol* 2010; **11**: 471–476.
38. Trzcinski K, Thompson C, Malley R, *et al.* Antibodies to conserved pneumococcal antigens correlate with, but are not required for, protection against pneumococcal colonization induced by prior exposure in a mouse model. *Infect Immun* 2005; **73**: 7043–7046.
39. Malley R, Trzcinski K, Srivastava A, *et al.* $CD^{4+}$ T cells mediate antibody-independent acquired immunity to pneumococcal colonization. *Proc Natl Acad Sci USA* 2005; **102**: 4848–4853.
40. Dintilhac A, Alloing G, Granadel C, *et al.* Competence and virulence of *Streptococcus pneumoniae*: Adc and PsaA mutants exhibit a requirement for Zn and Mn resulting from inactivation of putative ABC metal permeases. *Mol Microbiol* 1997; **25**: 727–739.

41. Grifantini R, Toukoki C, Colaprico A, *et al.* Peroxide stimulon and role of PerR in group A *Streptococcus*. *J Bacteriol* 2011; **193**: 6539–6551.
42. Krachler M, Rossipal E, Micetic-Turk D. Concentrations of trace elements in sera of newborns, young infants, and adults. *Biol Trace Elem Res* 1999; **68**: 121–135.
43. Martin JE, Lisher JP, Winkler ME, *et al.* Perturbation of manganese metabolism disrupts cell division in *Streptococcus pneumoniae*. *Mol Microbiol* 2017; **104**: 334–348.
44. Sharma A, Gaidamakova EK, Matrosova VY, *et al.* Responses of $Mn^{2+}$ speciation in *Deinococcus radiodurans* and *Escherichia coli* to gamma-radiation by advanced paramagnetic resonance methods. *Proc Natl Acad Sci USA* 2013; **110**: 5945–5950.
45. Culotta VC, Daly MJ. Manganese complexes: diverse metabolic routes to oxidative stress resistance in prokaryotes and yeast. *Antioxid Redox Signal* 2013; **19**: 933–944.
46. Barnese K, Gralla EB, Valentine JS, *et al.* Biologically relevant mechanism for catalytic superoxide removal by simple manganese compounds. *Proc Natl Acad Sci USA* 2012; **109**: 6892–6897.
47. Daly MJ, Gaidamakova EK, Matrosova VY, *et al.* Small-molecule antioxidant proteome-shields in *Deinococcus radiodurans*. *PLoS ONE* 2010; **5**: e12570.
48. Ogunniyi AD, Mahdi LK, Jennings MP, *et al.* Central role of manganese in regulation of stress responses, physiology, and metabolism in *Streptococcus pneumoniae*. *J Bacteriol* 2010; **192**: 4489–4497.
49. Hendriksen WT, Bootsma HJ, van Diepen A, *et al.* Strain-specific impact of PsaR of *Streptococcus pneumoniae* on global gene expression and virulence. *Microbiology* 2009; **155**: 1569–1579.
50. Kloosterman TG, Witwicki RM, van der Kooi-Pol MM, *et al.* Opposite effects of $Mn^{2+}$ and $Zn^{2+}$ on PsaR-mediated expression of the virulence genes *pcpA*, *prtA*, and *psaBCA* of *Streptococcus pneumoniae*. *J Bacteriol* 2008; **190**: 5382–5393.
51. Anderson RJ, Guru S, Weeratna R, *et al.* In vivo screen of genetically conserved *Streptococcus pneumoniae* proteins for protective immunogenicity. *Vaccine* 2016; **34**: 6292–6300.
52. Glover DT, Hollingshead SK, Briles DE. *Streptococcus pneumoniae* surface protein PcpA elicits protection against lung infection and fatal sepsis. *Infect Immun* 2008; **76**: 2767–2776.
53. Haneberg B, Herland Berstad AK, Holst J. Bacteria-derived particles as adjuvants for non-replicating nasal vaccines. *Adv Drug Deliv Rev* 2001; **51**: 143–147.
54. Blander JM, Medzhitov R. Toll-dependent selection of microbial antigens for presentation by dendritic cells. *Nature* 2006; **440**: 808–812.
55. Brodsky IE, Medzhitov R. Targeting of immune signalling networks by bacterial pathogens. *Nat Cell Biol* 2009; **11**: 521–526.
56. Zygmunt BM, Rharbaoui F, Groebe L, *et al.* Intranasal immunization promotes Th17 immune responses. *J Immunol* 2009; **183**: 6933–6938.
57. Dileepan T, Linehan JL, Moon JJ, *et al.* Robust antigen specific Th17 T cell response to group A Streptococcus is dependent on IL-6 and intranasal route of infection. *PLoS Pathog* 2011; **7**: e1002252.
58. Maroof A, Yorgensen YM, Li Y, *et al.* Intranasal vaccination promotes detrimental Th17-mediated immunity against influenza infection. *PLoS Pathog* 2014; **10**: e1003875.
59. Aguilo N, Alvarez-Arguedas S, Uranga S, *et al.* Pulmonary but not subcutaneous delivery of BCG vaccine confers protection to tuberculosis-susceptible mice by an interleukin 17-dependent mechanism. *J Infect Dis* 2016; **213**: 831–839.
60. Moffitt KL, Gierahn TM, Lu YJ, *et al.* T(H)17-based vaccine design for prevention of *Streptococcus pneumoniae* colonization. *Cell Host Microbe* 2011; **9**: 158–165.
61. Wilson R, Cohen JM, Jose RJ, *et al.* Protection against *Streptococcus pneumoniae* lung infection after nasopharyngeal colonization requires both humoral and cellular immune responses. *Mucosal Immunol* 2015; **8**: 627–639.
62. Wang Y, Jiang B, Guo Y, *et al.* Cross-protective mucosal immunity mediated by memory Th17 cells against *Streptococcus pneumoniae* lung infection. *Mucosal Immunol* 2017; **10**: 250–259.
63. Lu YJ, Yadav P, Clements JD, *et al.* Options for inactivation, adjuvant, and route of topical administration of a killed, unencapsulated pneumococcal whole-cell vaccine. *Clin Vaccine Immunol* 2010; **17**: 1005–1012.
64. Mutsch M, Zhou W, Rhodes P, *et al.* Use of the inactivated intranasal influenza vaccine and the risk of Bell's palsy in Switzerland. *N Engl J Med* 2004; **350**: 896–903.
65. Lewis DJ, Huo Z, Barnett S, *et al.* Transient facial nerve paralysis (Bell's palsy) following intranasal delivery of a genetically detoxified mutant of *Escherichia coli* heat labile toxin. *PLoS ONE* 2009; **4**: e6999.
66. Harvey RM, Ogunniyi AD, Chen AY, *et al.* Pneumolysin with low hemolytic activity confers an early growth advantage to *Streptococcus pneumoniae* in the blood. *Infect Immun* 2011; **79**: 4122–4130.
67. Fischer ER, Hansen BT, Nair V, *et al.* Scanning electron microscopy. *Curr Protoc Microbiol* 2012; Chapter 2: Unit 2B 2.
68. Daniels CC, Coan P, King J, *et al.* The proline-rich region of pneumococcal surface proteins A and C contains surface-accessible epitopes common to all pneumococci and elicits antibody-mediated protection against sepsis. *Infect Immun* 2010; **78**: 2163–2172.
69. McKenzie DR, Kara EE, Bastow CR, *et al.* IL-17-producing gammadelta T cells switch migratory patterns between resting and activated states. *Nat Commun* 2017; **8**: 15632.

## SUPPORTING INFORMATION

Additional supporting information may be found online in the Supporting Information section at the end of the article.